

AEROGEL

Marco Contalbrigo – INFN Ferrara

JLab, October 13th 2015



The CLAS12 large area RICH detector

M. Contalbrigo^{a,*}, E. Cisbani^b, P. Rossi^c

^a INFN Ferrara, Italy
^b INFN Roma and Istituto Superiore di Studi, Italy
^c INFN Laboratori Nazionali di Frascati, Italy

ARTICLE INFO

Available online 28 October 2010

Keywords:
RICH
CLAS12
Particle identification

ABSTRACT

A large area RICH detector is being designed as part of the Jefferson Lab Experiment identification from 3 GeV/c up to momenta design luminosity up to $10^{33} \text{ cm}^{-2} \text{ s}^{-1}$. The detector will consist of a highly segmented light detector in the visible wavelength range. The basic parameters of the RICH are outlined and the resulting performances, as defined by preliminary simulation studies, are reported.

© 2010 Elsevier B.V. All rights reserved.

lu:
the
nuck
show
solenoi
forward
polar ang
and retains

* Corresponding
E-mail address:
0168-9002/\$ - see front
doi:10.1016/j.nima.201

go@fe.infn.it (M. Contalbrigo).

© 2010 Elsevier B.V. All rights reserved.
447

Important observables that will be extensively investigated are transverse Momentum Distribution functions (TMDs) describing intrinsic spin-orbit effects and Generalized Parton Distribution functions (GPDs), containing information about the spatial distribution of quarks and the relation (by a sum rule) to the elusive intrinsic orbital momenta. Several experiments have been already performed by the JLab12 PAC to study kaon versus pion production in exclusive and semi-inclusive scattering, providing access to the decomposition of the two sets of non-perturbative wave functions. The main features of CLAS12 include a high operational luminosity of $10^{33} \text{ cm}^{-2} \text{ s}^{-1}$, an order of magnitude higher than the existing setup, and operation of highly polarized beam and target. The conceptual design of the CLAS12 detector is shown in Fig. 1. The central detector with the high-field (5 T) torus magnet is used for particle tracking at large angles. The large area RICH detector detects charged and neutral particles in the momentum range between 5 and 40 GeV/c. It employs a 2 T torus magnet geometry to maintain the detector symmetry of CLAS. In the base equipment,

rejection factor of 10^4 is required to achieve the desired particle identification and event reconstruction. This can be achieved in this momentum range by replacing the existing low-threshold Cherenkov counter (LTCC) with a RICH detector without any impact on the baseline design of CLAS12.

tion and event reconstruction can be achieved in this momentum range by replacing the existing low-threshold Cherenkov counter (LTCC) with a RICH detector without any impact on the baseline design of CLAS12.

2. The CLAS12 RICH

To fit into the CLAS12 geometry, the RICH should have a projective geometry with six sectors that cover the space between the torus cryostats and covering scattering angles from 10° to 40° . Fig. 3. Being downstream to the torus magnet at the interaction point, the RICH has to cover a large area of each sector spanning an area of the order of 4 m^2 . Being located between detectors which are already in the construction, the RICH gap depth cannot exceed 1 m. The proposed solution is a segmented focusing RICH.

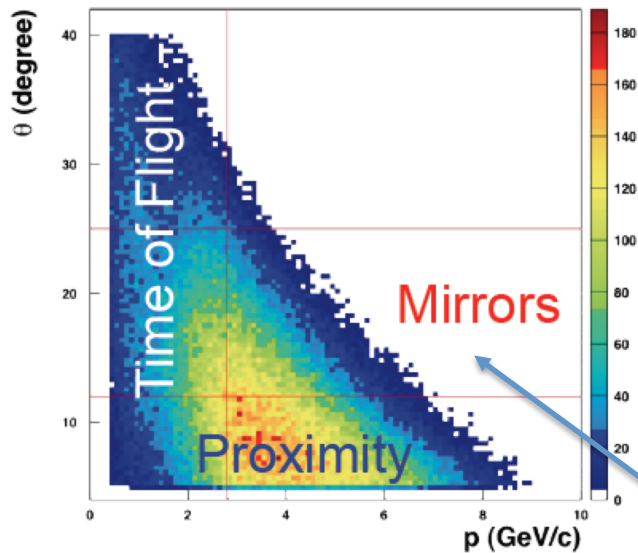
A setup similar to the one adopted in Hall-B at JLab, using a C_5F_{12} or C_6F_{14} radiator and a CsI-deposited radiator chamber as a UV-photon detector, is required to achieve the required pion rejection factor at momenta up to 40 GeV/c.

The preliminary results on ongoing Monte Carlo studies, based on a GEANT3 toolkit with simplified geometry, show that a RICH with a freon wire proportional counter can achieve the required pion rejection factor at momenta up to 40 GeV/c.

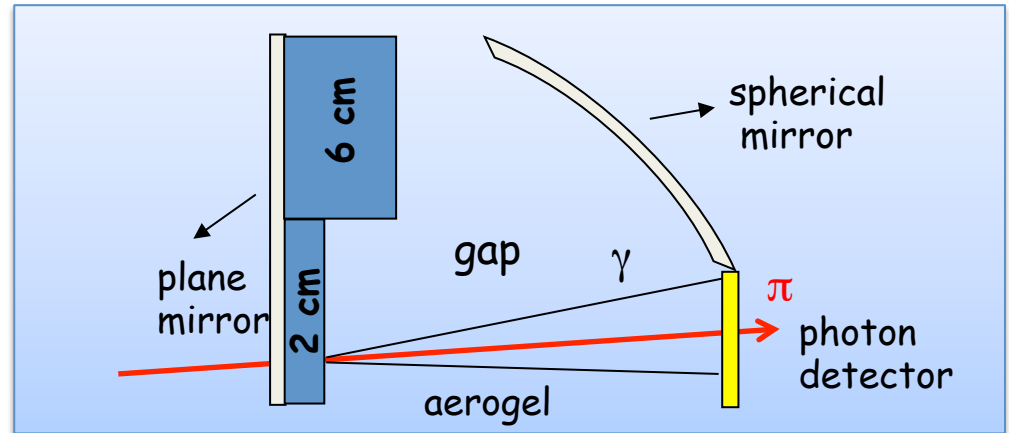
1
ce
m
face,
ained
ase, the
ximity

with a freon
wire propor-
t achieve the
than 3 GeV/c.
o studies, based
nd optical surface

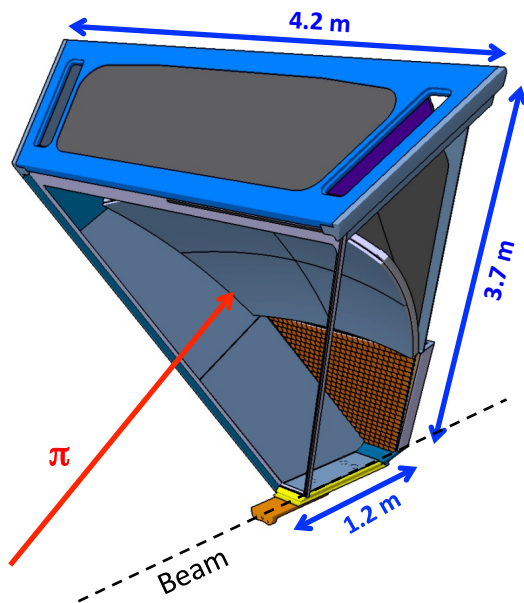
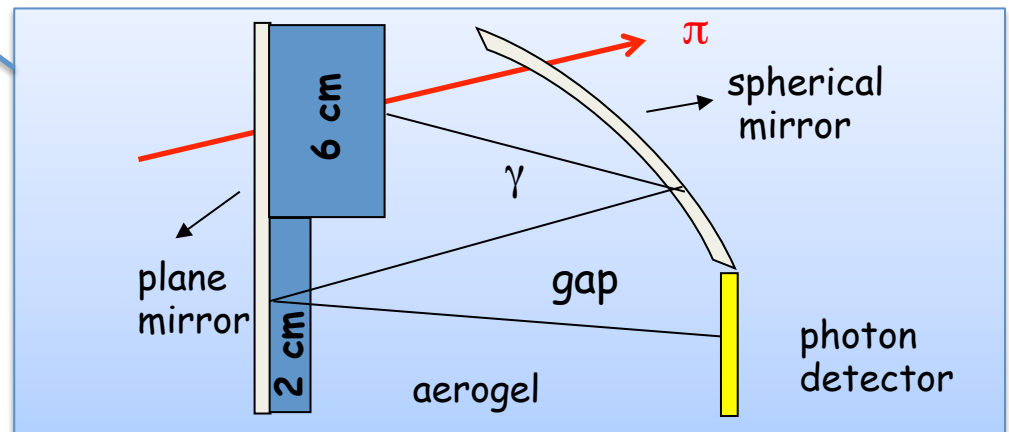
The Hybrid Optics Design



Direct rings and best performance for high momentum particles



Reflected rings for less demanding low momentum particles



- Minimize active area (cost) to about 1 m²
- Material budget concentrated where TOF is less effective
- Focalizing mirrors allow thick radiator for good light yield
- Time resolution < 1 ns to distinguish direct and reflected patterns

Aerogel Production

First 3 cm thick layer (44 tiles) under production since November 2014

Initial goal: 25 % production efficiency

Initial performance (up to 8/15):

- ~ 2 months delay for initial lack of chemicals
- ~ 3 months to finalize acceptance test procedure

- 7 batches in ~4 months
 - 105 tiles synthesized
 - 50 tiles without cracks
 - 18 tiles within specifications



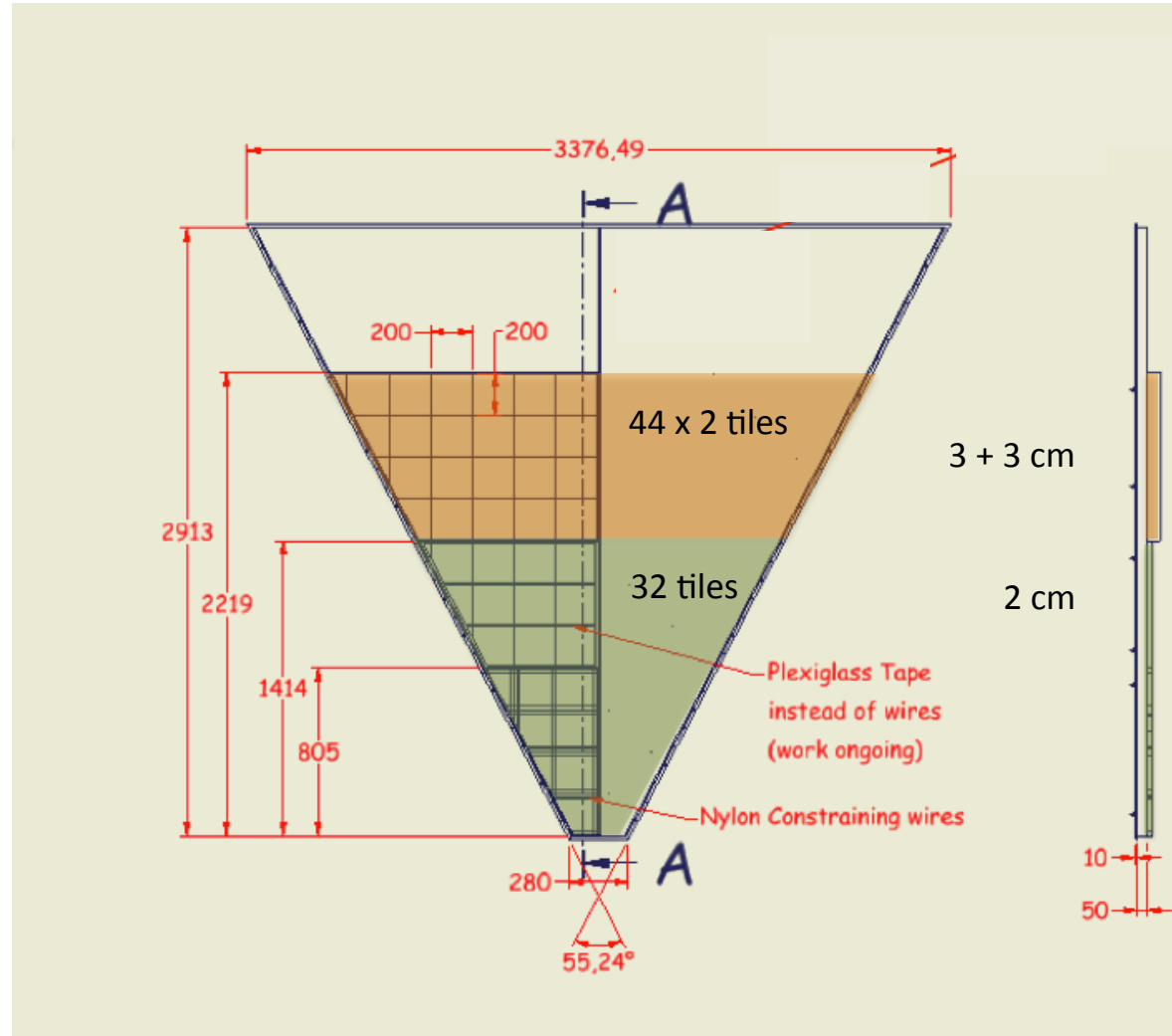
Production rate capability

2 batches/month

Production efficiency

2.5 tiles/batch -> 17 % (conservative)

21 months up to completion



Aerogel Specifications

OPTICAL:

Density	$0.223 < \rho < 0.245$	gr/cm ³
Refractive index	$(n^2=1+0.438 \rho)$	$1.0477 < n < 1.0523$
Scattering length	$L_{sc} > 43$	mm
Absorption coefficient	$A > 0.95$	

MECHANICAL:

Side to side length variation $\Delta L_{side} < 0.25$ mm
from diamond wire to diamond wheel for better precision

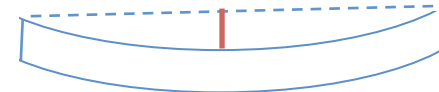


Tile to tile thickness variation $\Delta H_{tile} < 1.5$ mm

disregard molds with bad performance

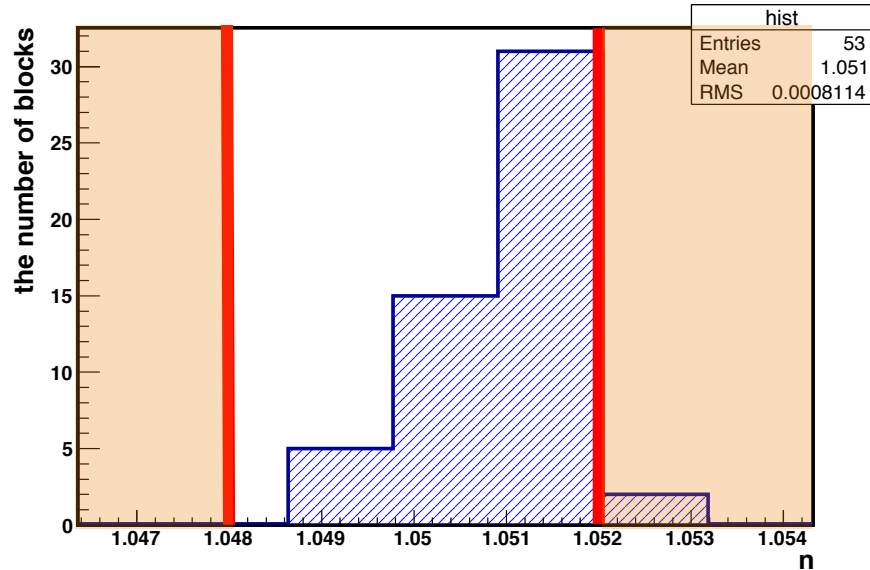


Surface planarity $\Delta S_{surf} < 1.5$ mm

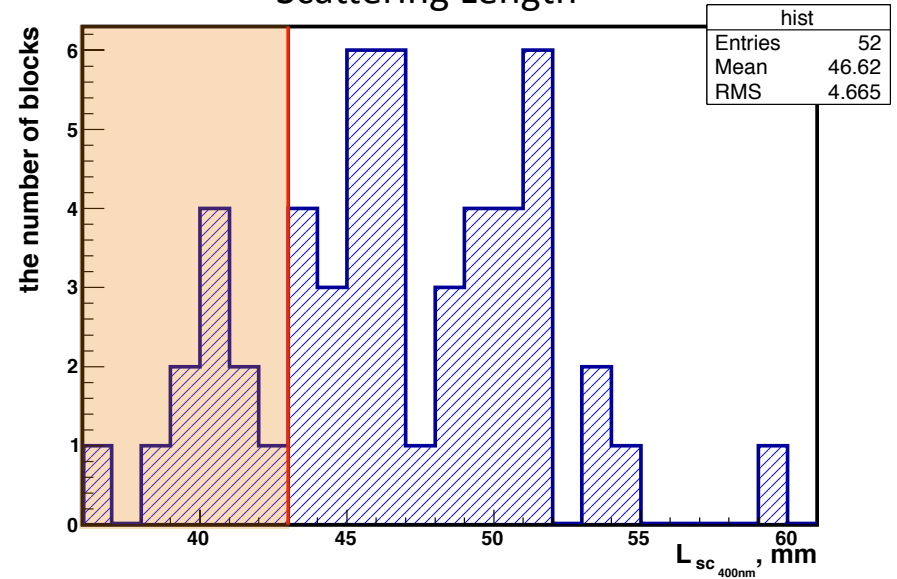


Aerogel Specifications

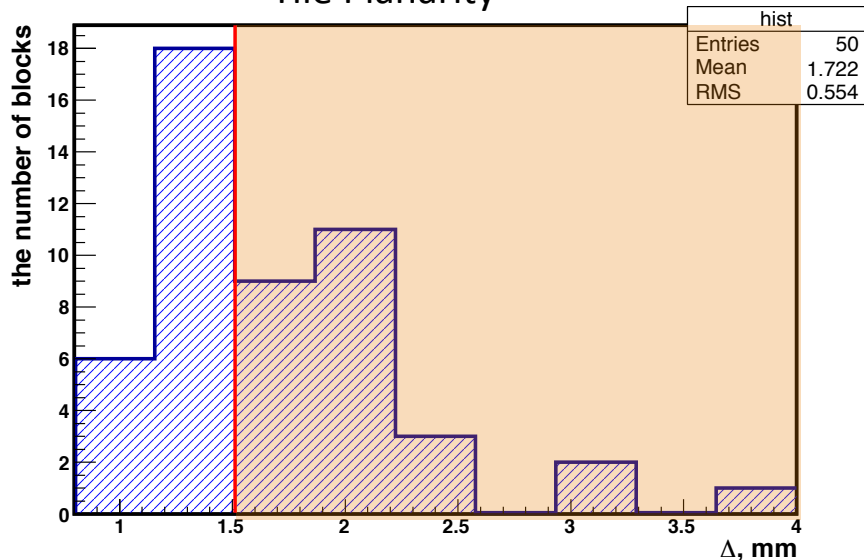
Refractive Index



Scattering Length



Tile Planarity



Homogeneous refractive index ✓

20 % losses due to scattering length ✓

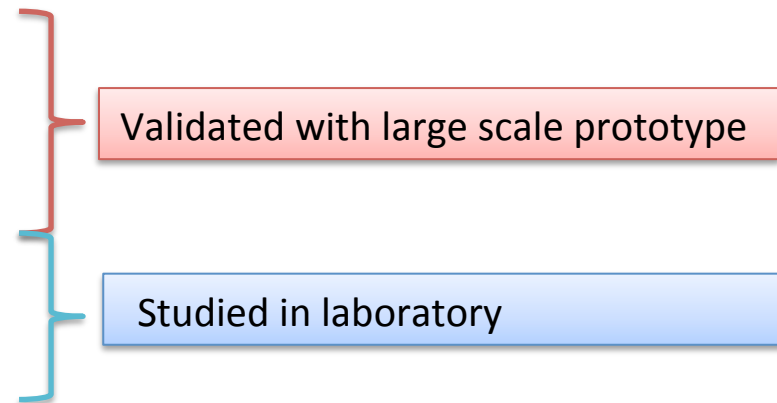
Average Scattering Length $L_{sc} = 48.3$ mm

50 % losses due to planarity ✓

Mitigation actions: relax planarity specifications
- increase the production efficiency close to 25 %

CLAS12 RHIC: Resolution

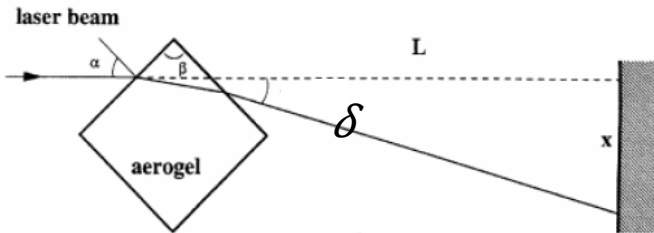
Resolution	Direct (mrad)	Reflected (mrad)
Emission Point	1.7	1.7
Readout Accuracy	2.1	1.0
Chromatic Aberration	3.0	2.5
Aerogel Optical Prop.	≤ 1	≤ 2
Mirror System		≤ 1
σ_{θ} (1 p.e.)	4.2	3.9
Requirements	Direct	Reflected
Max. momentum	8 GeV/c	6 GeV/c
σ_{θ} (4 σ separation)	1.4 mrad	2.5 mrad
Np.e. Yield	≥ 10	≥ 3



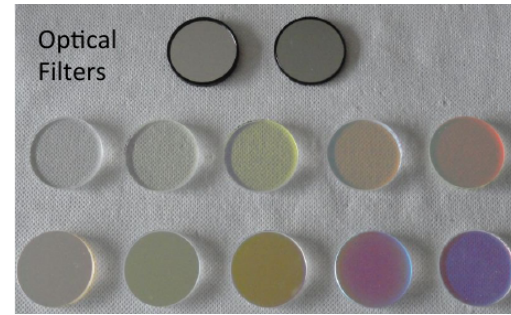
$$\sigma_{\vartheta_{Ch}} = \sqrt{\frac{\sum_i (\sigma_{\vartheta_{Ch}}^i)^2}{N_{p.e.}}}$$

Aerogel Chromatic Dispersion

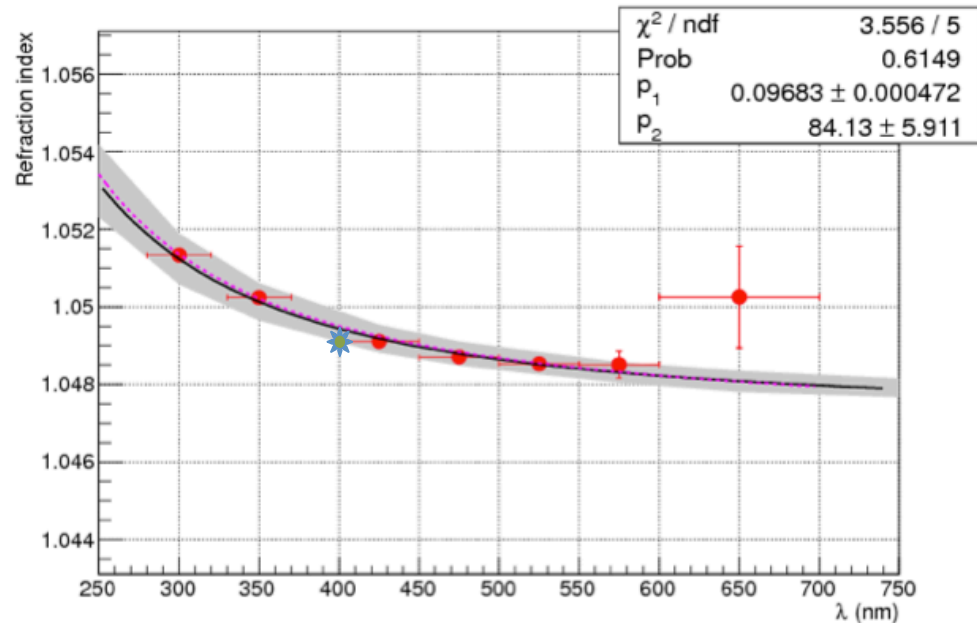
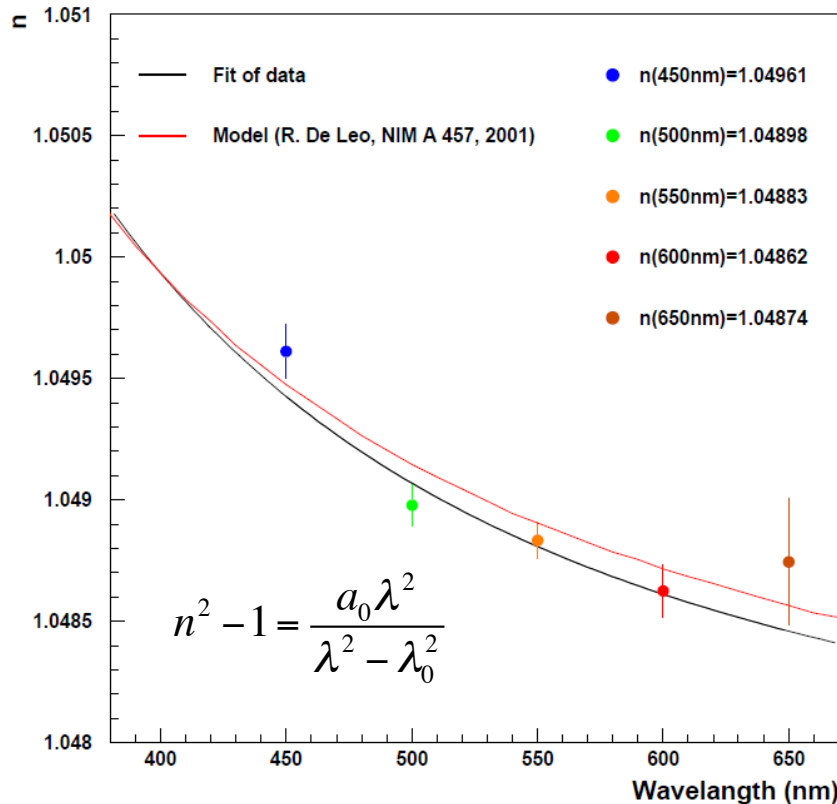
Measured by prisma method:



Measured by prototype with optical filters:



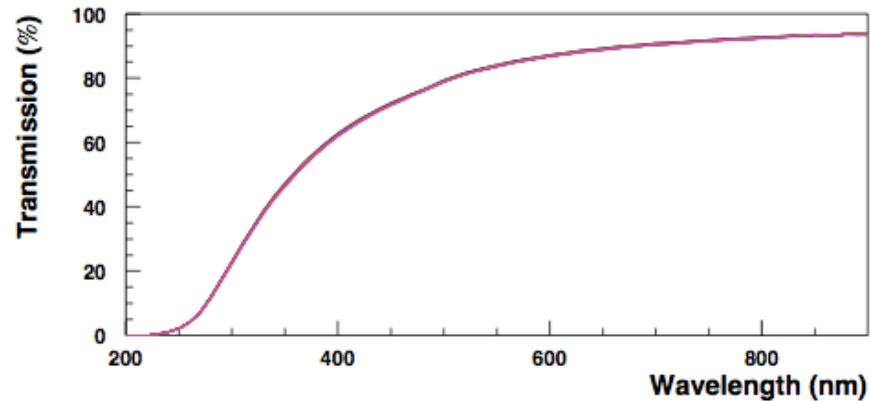
Chromatic dispersion



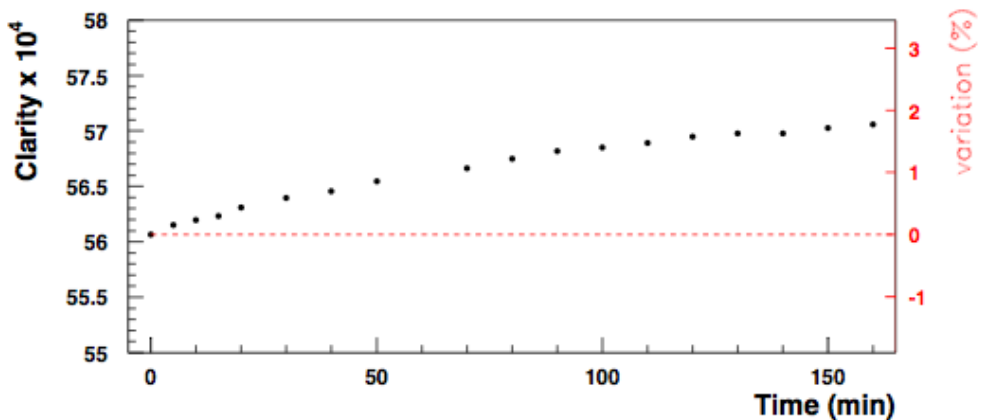
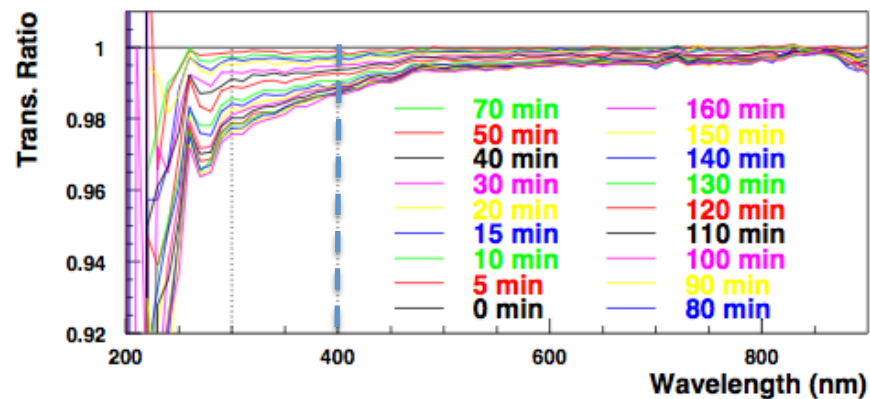
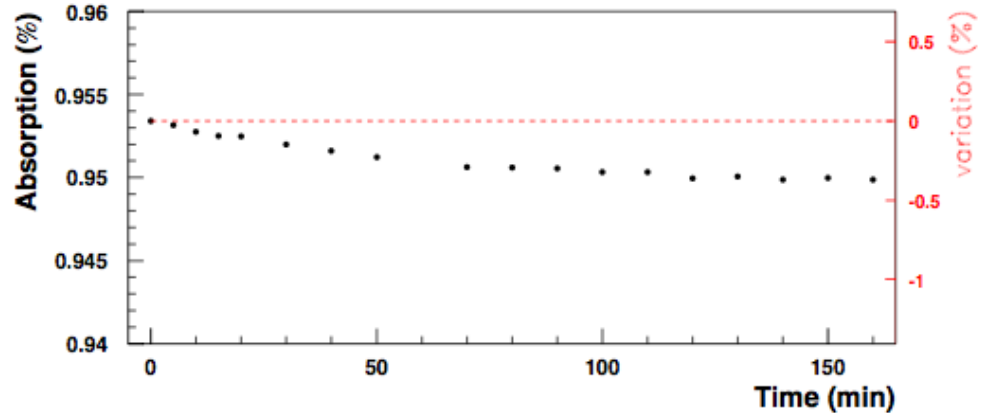
Expected value from density:
 $n(400\text{nm}) = [1 + 0.438\rho]^{1/2} = 1.0492$

Aerogel Characteristics in the Air

Transmission vs Time

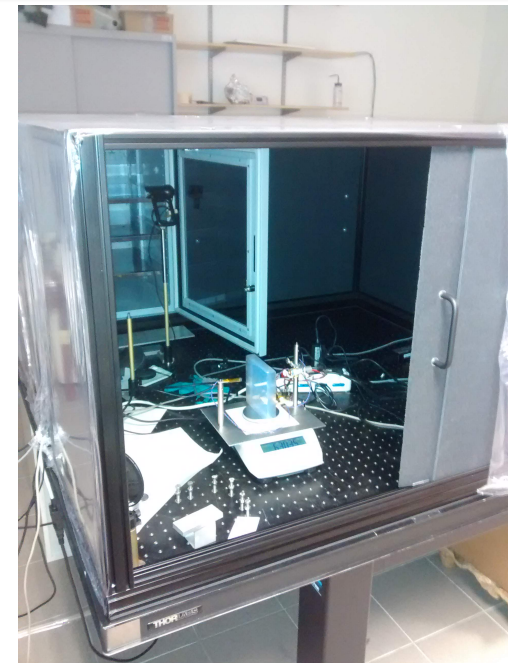
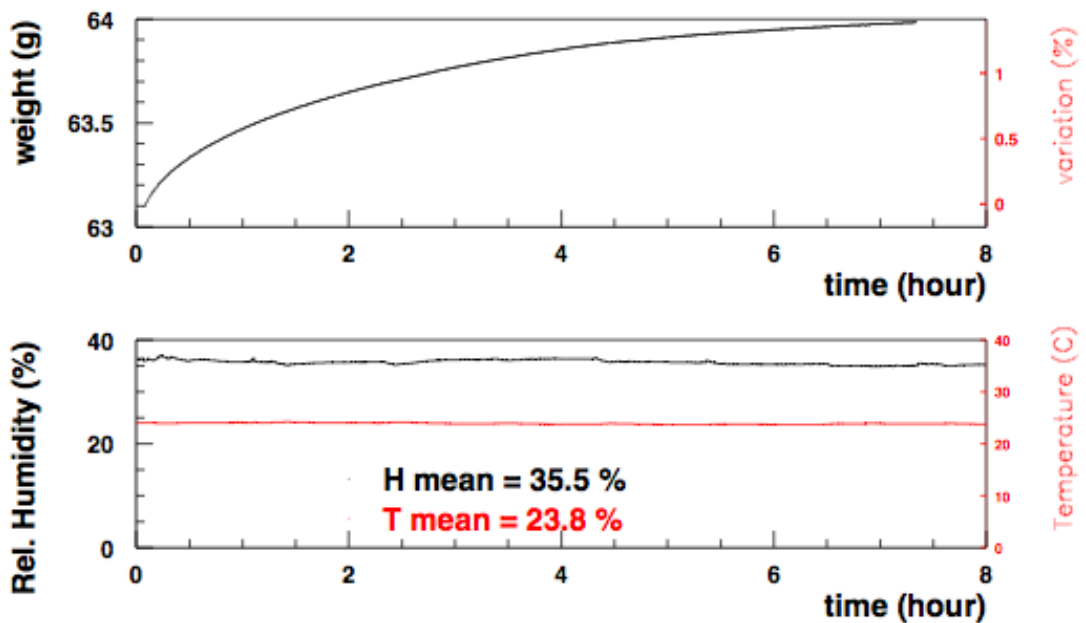


Absorption and Clarity @ 400 nm



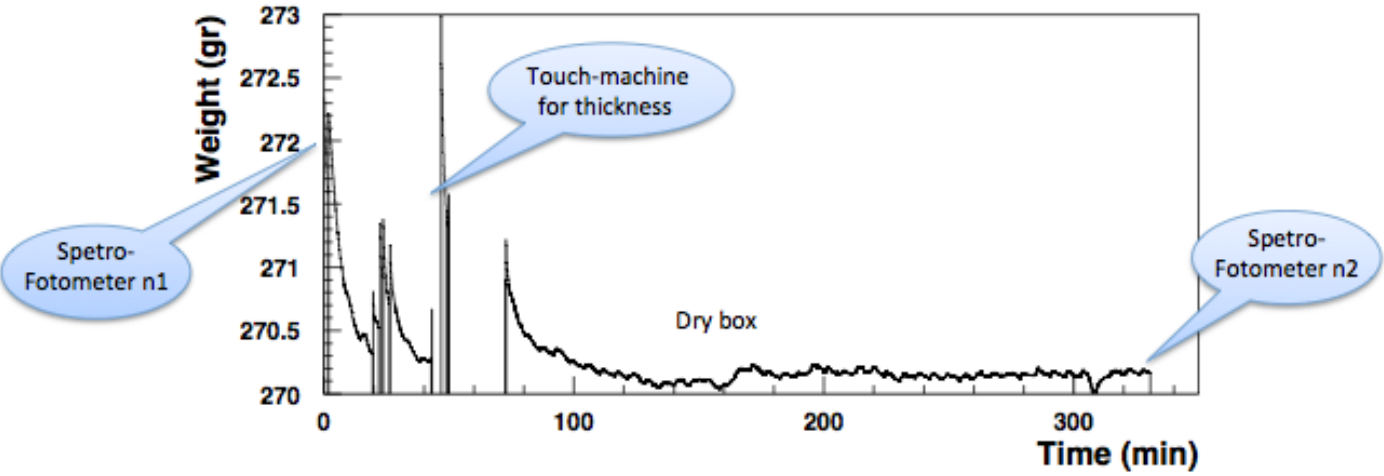
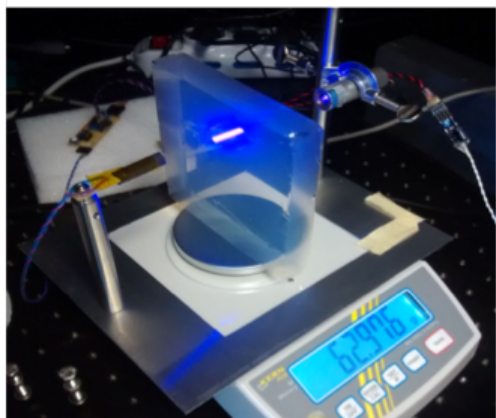
Monitoring the time dependence of the transmission of aerogel tile in environment of non-zero relative humidity (~ 40 %)

Aerogel Weight



In Air (≈ 40 % RH)

Inside Dry-Box (≈ 1 % RH)



Aerogel Storage



Within sealed envelopes

Inside a dry-cabinet (few % RH)



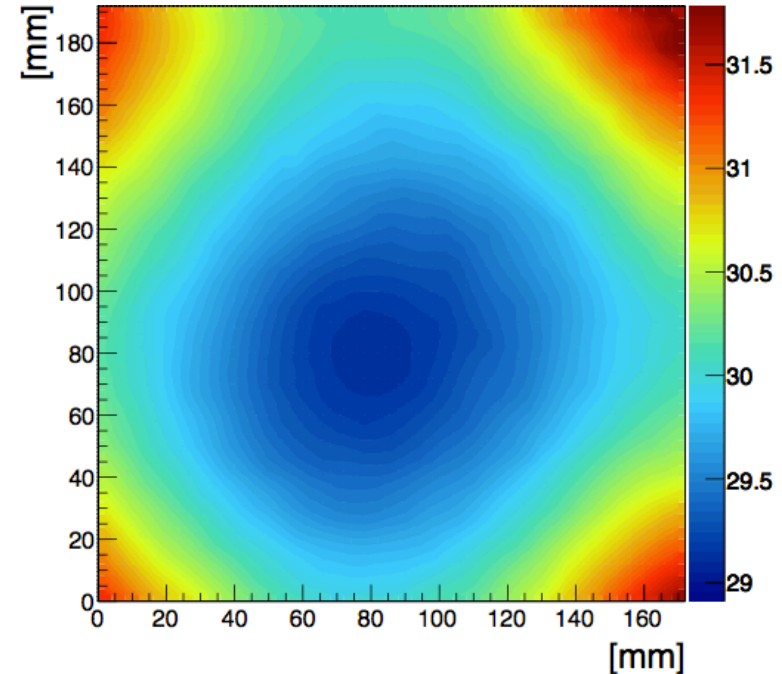
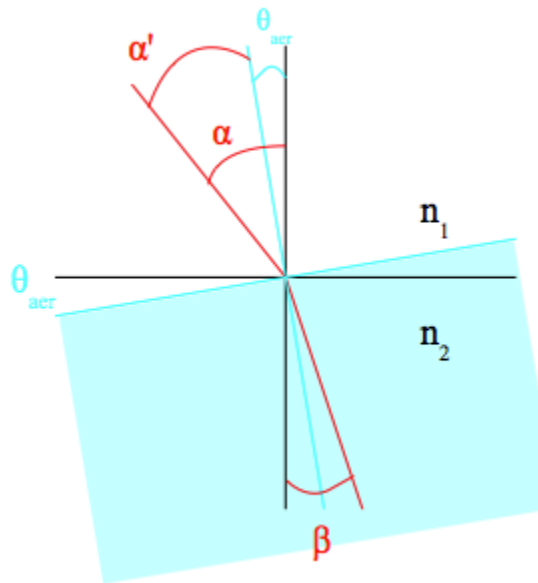
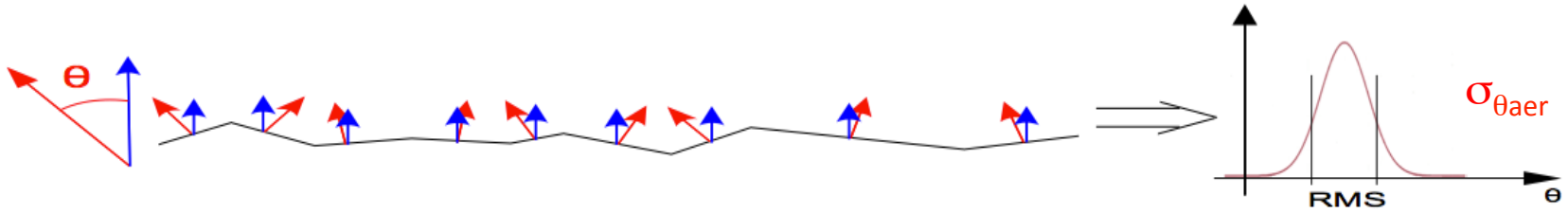
Spectro-fotometer Measurements

Acceptance tests during vendor visit in Ferrara (April 2015)

		Novosibirsk	Fe re-fit	Ferrara 1	Ferrara 2
	Date Meas.	28 Dec 2014	28 Dec 2014	16 Apr 2015 after delivery	17 Apr 15 after -1day drying
397m10	Lsc (mm)	49.2 ± 1.5	48.46 ± 0.50	45.59 ± 0.38	45.99 ± 0.39
	Abs (%)	97.7 ± 0.9	98.06 ± 0.61	95.60 ± 0.98	95.60 ± 1.06
	Date Meas.	20 Jan 2015		14 Apr 2015 after delivery	28 Apr 15 after 10-day drying
398m3	Lsc (mm)	40.93 ± 0.51		37.35 ± 0.47	37.59 ± 0.47
	Abs (%)	98.35 ± 0.7		96.37 ± 1.41	96.50 ± 1.36
	Date Meas.	28 Dec 2014	28 Dec 2014		
397m0	Lsc (mm)	48.20 ± 0.63	48.01 ± 0.42		
	Abs (%)	92.98 ± 0.5	93.05 ± 0.37		
	Date Meas.	22 Apr 2015 after trip to Novo	22 Apr 2015 after trip to Novo	16 Apr 2015 pre-baking	17 Apr 15 after baking
NOV LNF2 t1	Lsc (mm)	50.35 ± 0.36	49.79 ± 0.18	44.64 ± 0.63	49.62 ± 0.46
	Abs (%)	96.08 ± 0.05	96.26 ± 0.06	96.59 ± 0.42	96.59 ± 0.47

Result: Russian vendor agrees to bake twice: after production and before delivering

Aerogel Surface Quality



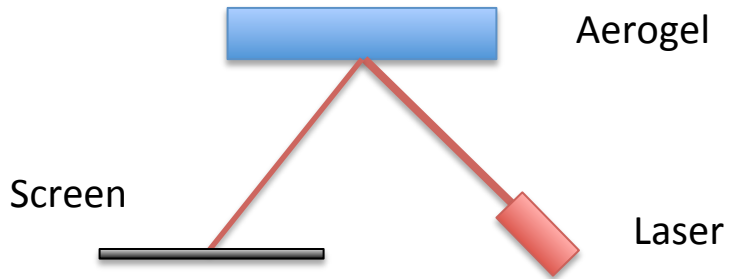
Refraction from a surface with local normal deviation θ

$$\beta = \vartheta_{aer} + \arcsin\left(\frac{1}{n} \sin(\alpha - \vartheta_{aer})\right)$$

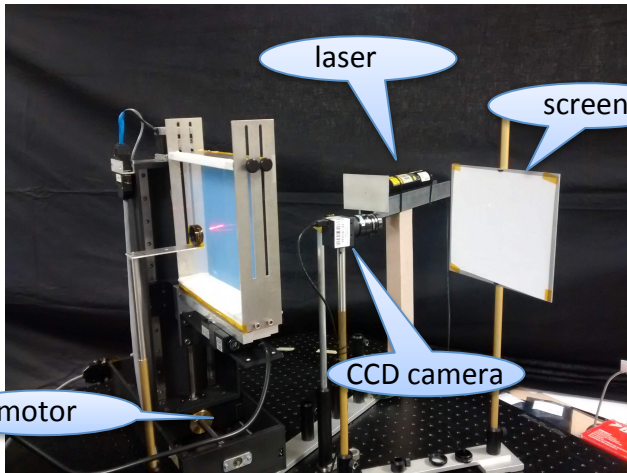
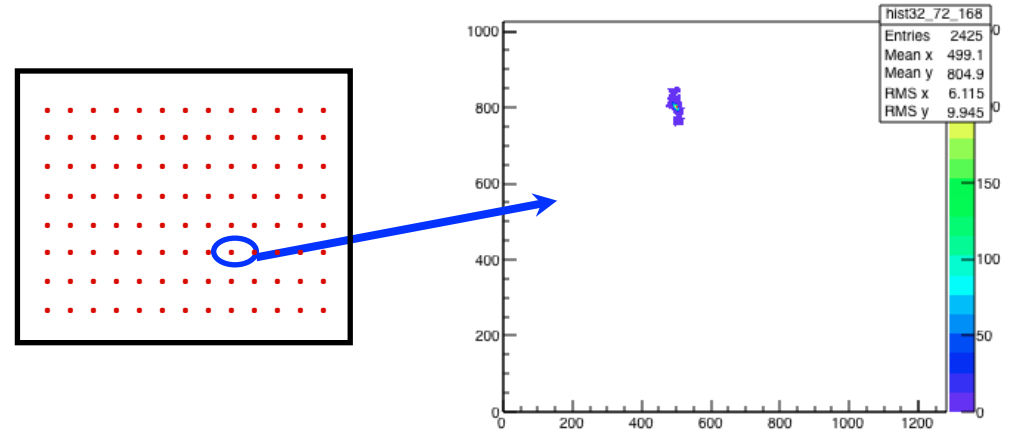
Contribution on light dispersion at small incident angles

$$\sigma_{\vartheta_{light}} = \left(1 - \frac{1}{n}\right) \cdot \sigma_{\vartheta_{aer}} \approx 0.05 \cdot \sigma_{\vartheta_{aer}}$$

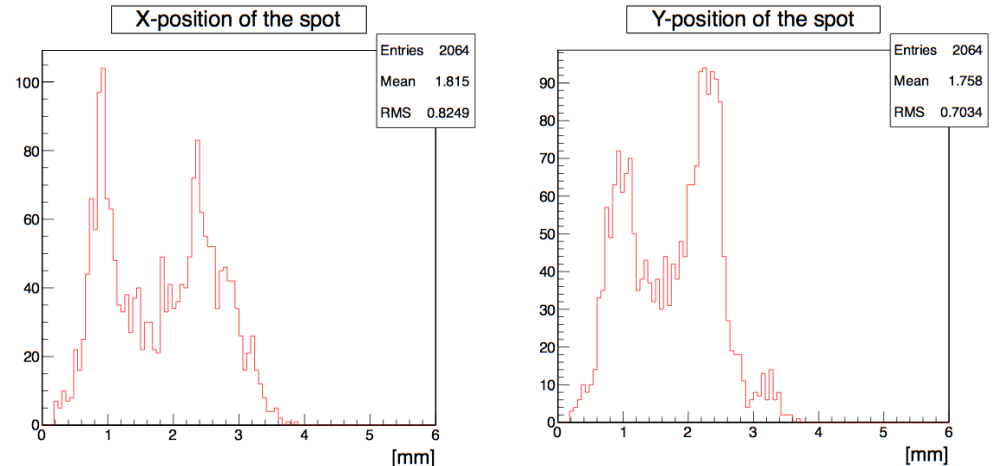
Aerogel Surface Scan



Scan of aerogel surface



Distributions of X & Y positions of the spot



x-y axis movable table

CCD camera [ThorLabs DCU 224c]
- sensitive area [5.95-4.76 mm]
- resolution [1280-1024 pixels]
- pixel size 4.65 μm

Aerogel Surface Planarity

From laser spot shifts to surface gradients

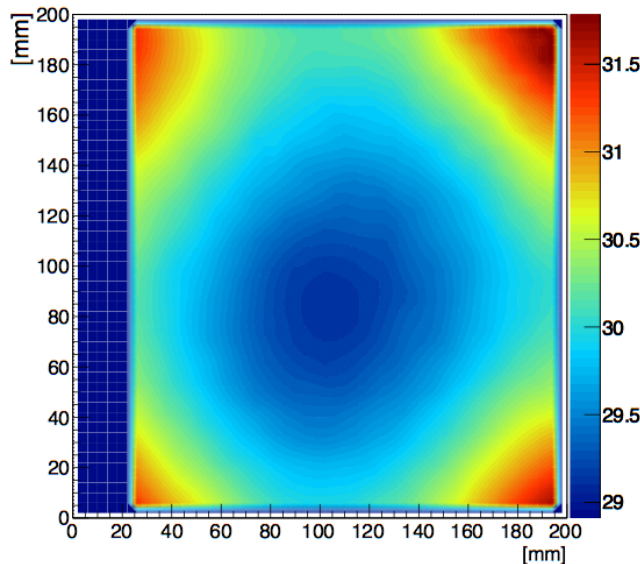
$$\nabla_x = \frac{(x - x_{mean})c_l}{2L} \cos(\theta)$$

$$\nabla_y = \frac{(y - y_{mean})c_l}{2L}$$

$$L = R/\cos(\theta)$$

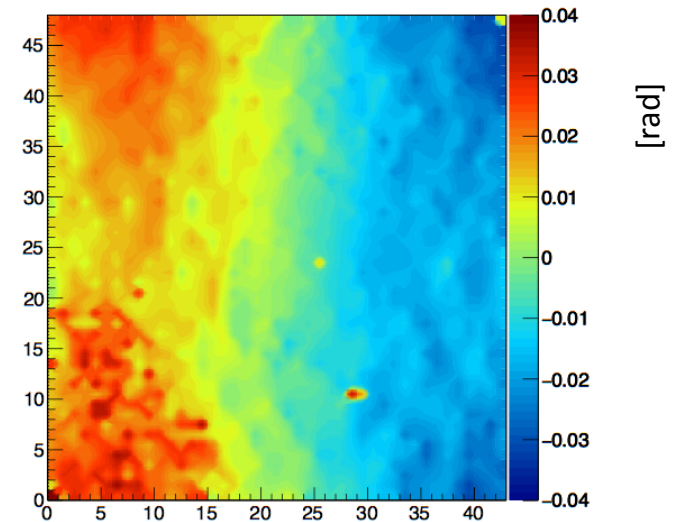
From surface gradients to surface map by linear regression

Surface map 10°

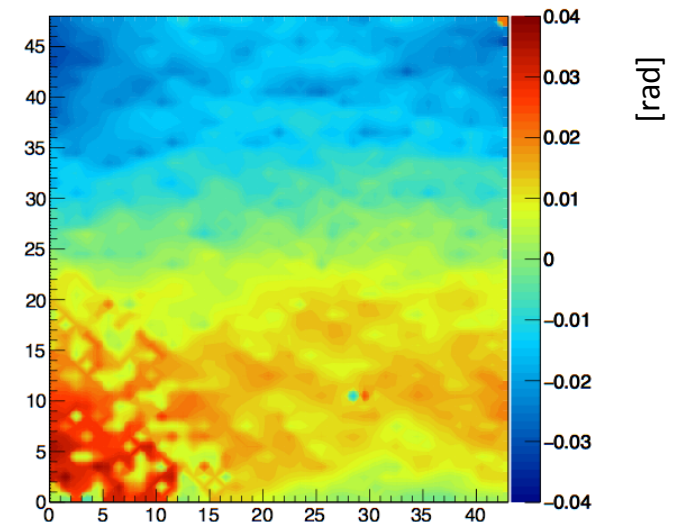


Validated with touch machine measurements
Consistent with Russian vendor planarity evaluation

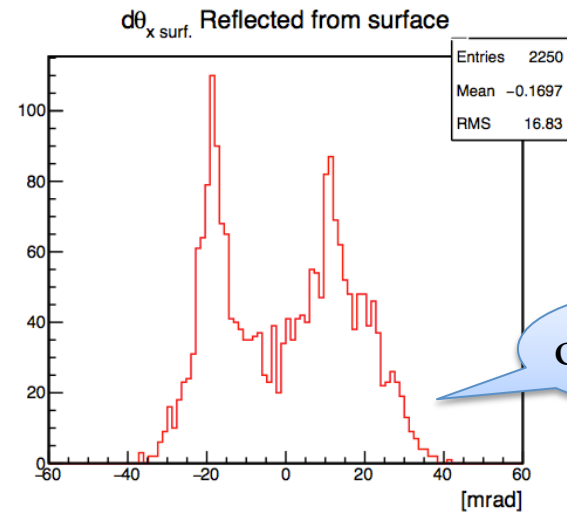
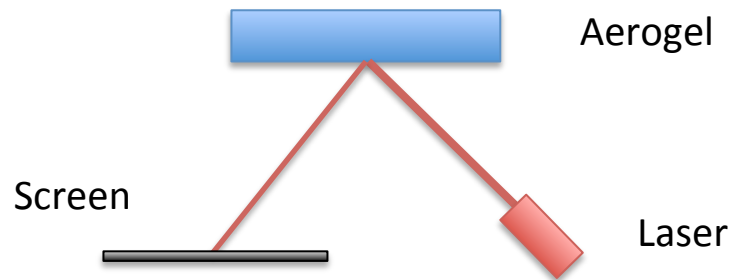
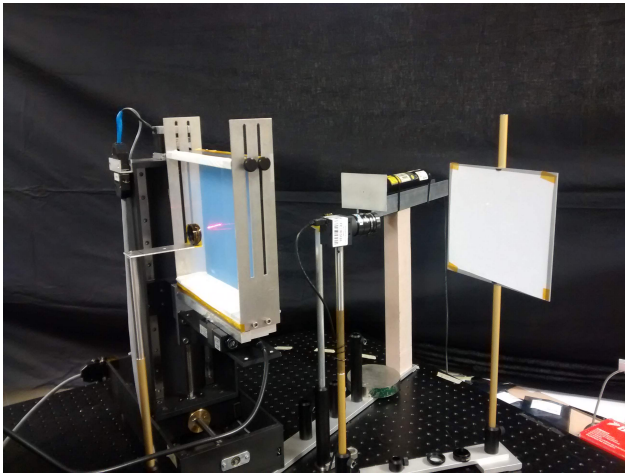
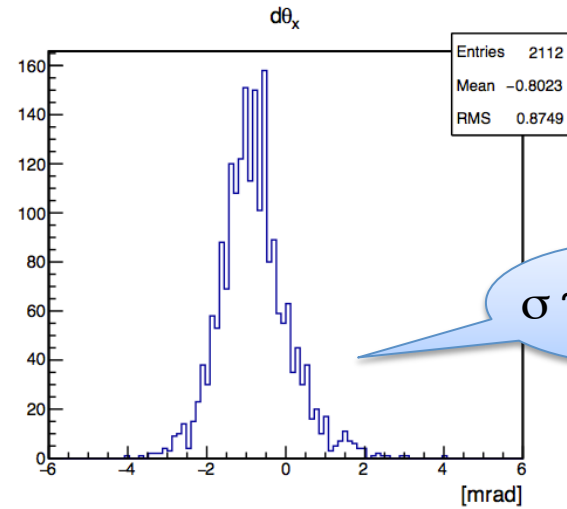
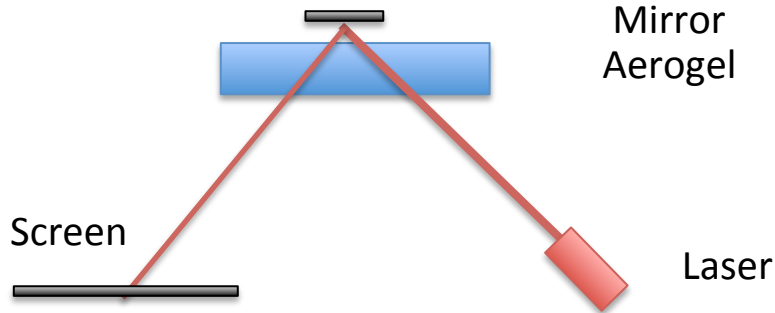
X-gradient



Y-gradient



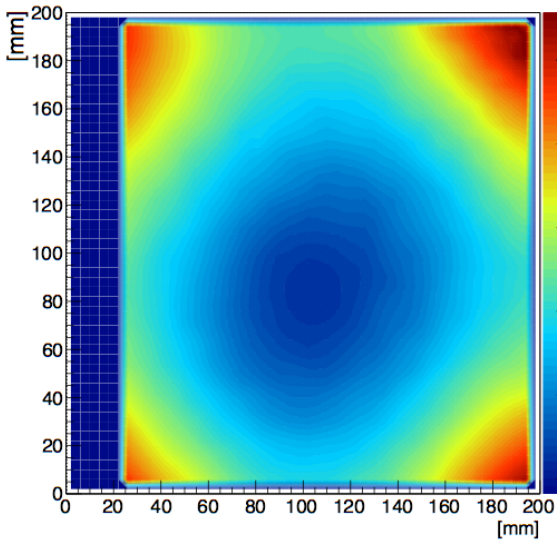
Light Dispersion vs Aerogel Surface Quality



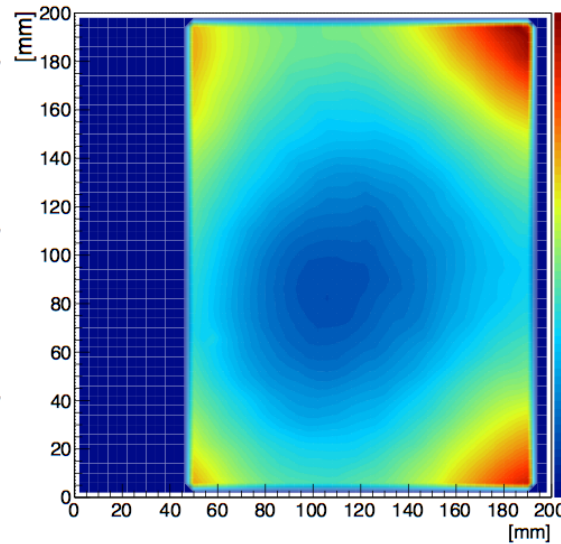
Acceptable light dispersion
up to $\Delta S_{\text{surf}} = 2.5$ mm planarity

Aerogel Surface Map

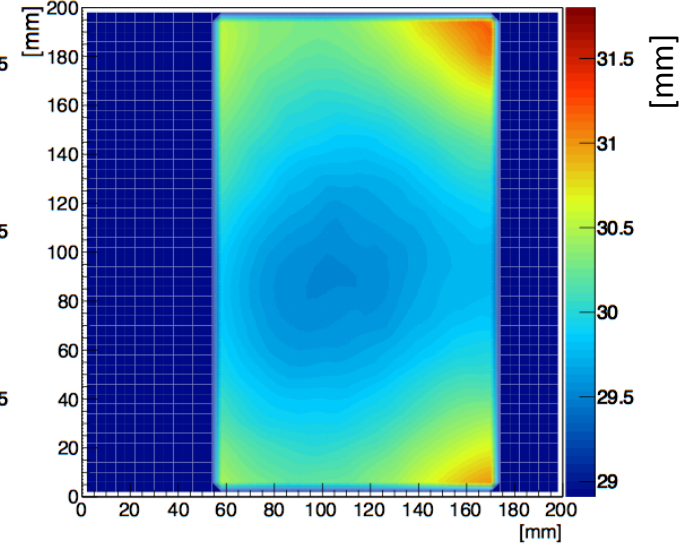
Surface map 10°



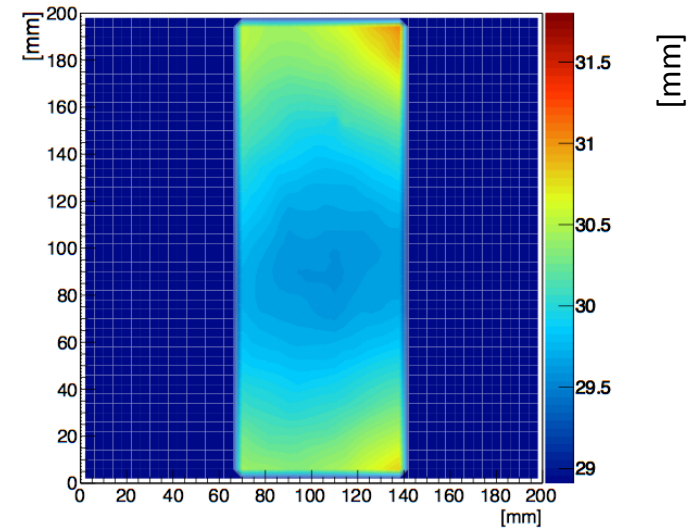
Surface map 20°



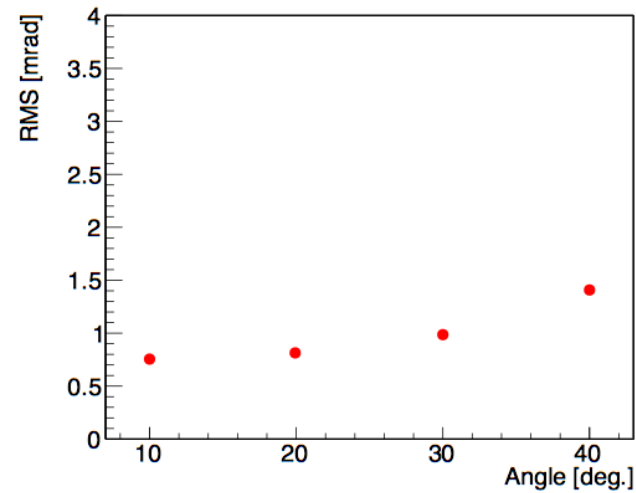
Surface map 30°



Surface map 40°

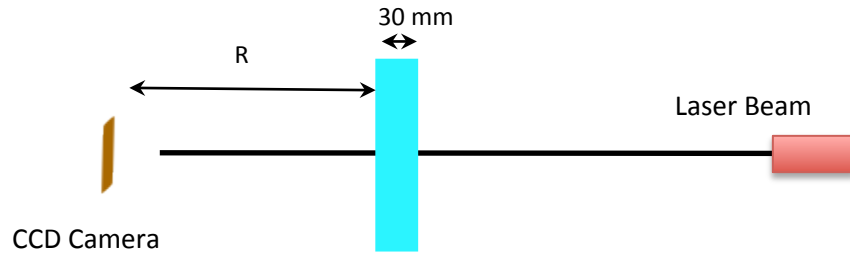


Light dispersion as a function of incident angle:



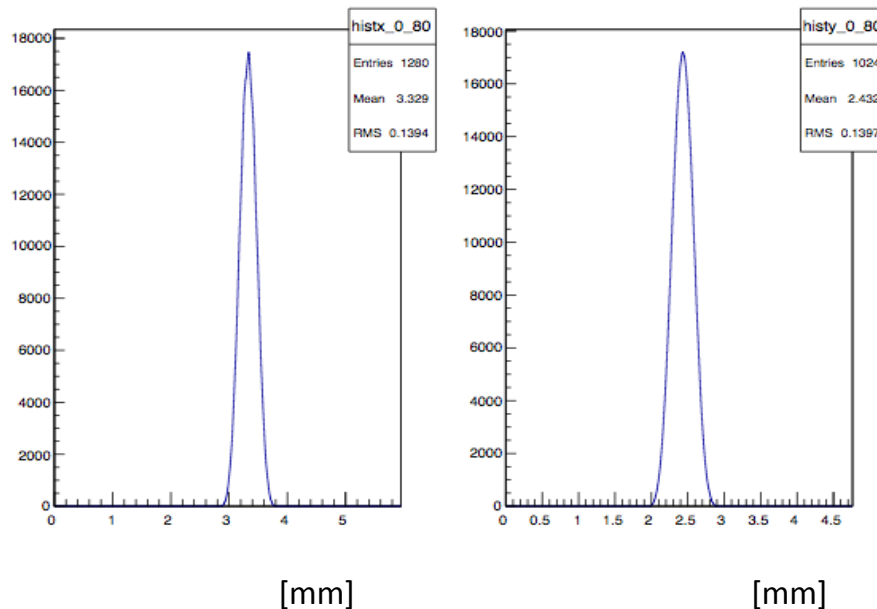
Forward Scattering

Description of the setup



Scattering of the light in the medium due to the anisotropy of the dielectric properties caused by density microscopic fluctuations

Examples of X & Y profiles of the spot

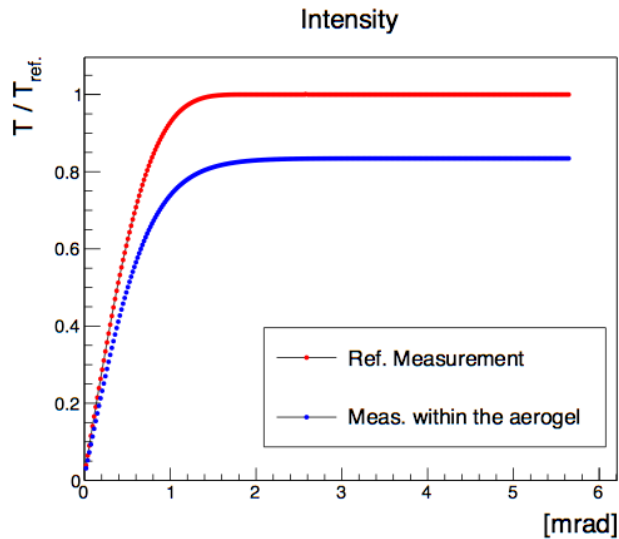


Analysis steps:

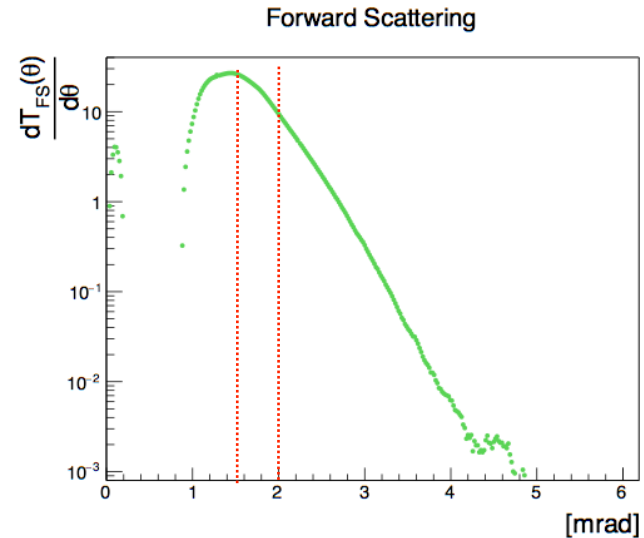
- Reference beam profile taken without aerogel
- Extract laser beam profile and compare with reference measurement
- Extract angular dependence of light intensity after passage through the aerogel

Forward Scattering

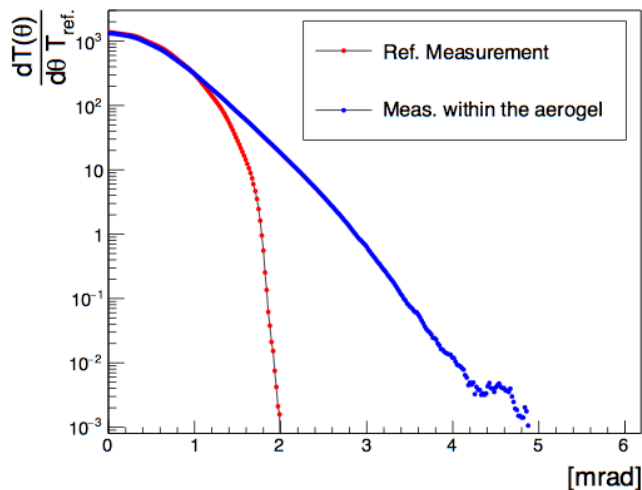
Angular dependence of the measured intensity:



$$\frac{dT_{FS}(\theta)}{d\theta} = \frac{dT(\theta)}{d\theta} \frac{1}{T_{ref.}} - \frac{T_0(\theta)}{d\theta} \frac{1}{T_{ref.}}$$



Differential of the measured intensity:



$$\frac{\int_2^6 T(\theta) d\theta}{\int_0^6 T(\theta) d\theta} \rightarrow 0.6\% \qquad \frac{\int_{1.5}^6 T(\theta) d\theta}{\int_0^6 T(\theta) d\theta} \rightarrow 2.7\%$$

Negligible scattering
at angles relevant for Cherenkov resolution

Conclusions

Aerogel production is ongoing

- ✓ Good average optical quality
- ✓ Suboptimal 17% production efficiency



Dedicated measurements indicates the planarity requirement is too stringent
It will be released to achieve the expected 25 % production efficiency

- ✓ Tools for measurements and monitoring of the aerogel characteristics are operational and have stable performance.
- ✓ Mismatch between the measurements done in Novosibirsk and in Ferrara was observed, indicating the necessity to bake the aerogel before delivery. Corresponding agreement was obtained with the producer.
- ✓ Storing (in dry cabinets) and handling procedures has been defined